Spectroscopy of π bonding in hard graphitic carbon nitride films: Superstructure of basal planes and hardening mechanisms

I. Jiménez, R. Gago, and J. M. Albella
Instituto de Ciencia de Materiales de Madrid (CSIC) Campus de Cantoblanco 28049 Madrid, Spain

D. Cáceres and I. Vergara
Departamento de Física Aplicada, Universidad Carlos III de Madrid, 28911 Leganés, Spain

(Received 4 May 2000)

X-ray-absorption near-edge spectroscopy (XANES or NEXAFS) has been used to obtain information on the orientation, corrugation, and cross-linking of graphitic carbon nitride planes, structural parameters that determine the mechanical properties of the material. The contribution of *p* electrons from carbon and nitrogen atoms to π bonding in graphitic carbon nitride has been studied with elemental and angular sensitivity by XANES. The density of π^* states from nitrogen is composition dependent and presents angular anisotropy, while the density of π^* states from carbon is isotropic and independent of composition. Both observations are consistent with a model of the superstructure of basal planes.

Carbon nitride films have been the aim of intense research since the theoretical work of Cohen and Liu predicting a β-C_3N_4 phase harder than diamond.[1] However, most of the attempts to synthesize this phase have resulted in the growth of amorphous graphitic films with a nitrogen content below 50 at. %.[2] These experimental results have stimulated theoretical work on graphitic carbon nitrides, both on hypothetical crystalline phases[3] and on amorphous structures.[4–7]

An important finding with regards to graphitic structures is that the orientation and cross-linking of basal planes improves significantly the hardness and elasticity of the material.[8] The orientation, corrugation, folding, and cross-linking of basal planes give shape to a superstructure that determines the actual physical properties of the graphitic solid. This result seems valid for other laminar materials, similarly to what is found with fullerenelike structures.[9]

Obtaining information on the superstructure is a difficult task since, on the one hand, it lacks long-range order and, on the other hand, the bonding structure remains essentially graphitic. Hitherto, only high-resolution transmission electron microscopy has been capable of detecting the superstructure of graphitic planes.[8] Here, we present an analysis of π^* states measured by x-ray-absorption spectroscopy (XANES) that provides a link between the bonding and electronic structure and the geometry of the superstructure.

Previous work on graphitic carbon nitride has reported a decrease of the electric charge in π bonds with increasing nitrogen content[6,10] that was explained by the curvature induced in the basal planes due to the presence of nitrogen. Some authors consider that the presence of nitrogen is enough to explain the bending of basal planes formed only by six-member rings, and that the cross-linking of different planes can go through threefold coordinated sp^2 hybridized carbon atoms.[7] Other authors consider that it is necessary to include five-member rings in the basal planes to explain their curvature, and that cross-linking takes place through fourfold-coordinated sp^3 hybridized atoms, either carbon[8,10] or nitrogen.[11] Discerning the mechanism ruling the bending and cross-linking of basal planes seems of major interest to understand the properties of graphitic carbon nitride.

This question can be answered by studying the contribution to π bonding of electrons from C and N atoms separately. A well-suited technique is x-ray-absorption near-edge spectroscopy (XANES), where electrons from 1*s* core levels of the different atoms are promoted to unoccupied states, preferentially of π^* character due to the dipolar transition rules. In addition, the XANES spectral features of C(1*s*) and N(1*s*) are much narrower and better resolved than those for other core-level spectroscopies such as photoemission.[12] Previous XANES measurements have repeatedly found a significant proportion of π^* states both on the C(1*s*) and N(1*s*) spectra.[13–16] However, a detailed composition- and angle-dependent XANES study was lacking.

We have prepared amorphous carbon nitride films on clean *p*-type (100) Si substrates by evaporating graphite lumps with concurrent bombardment of nitrogen ions. Graphite was evaporated with an electron gun at a rate of $\sim$3 Å/s. Different nitrogen content values were achieved by varying the ion energy and current density, although always limited to $[N]/[C]<0.3$. The typical film thickness was $\sim$300 nm.

The XANES measurements were performed at the SACEMOR endstation (beam line SA72) of the LURE synchrotron facility. The data were acquired in the total-yield mode by collecting with a channeltron the electron emission from the sample, and were normalized to the signal from a gold-covered grid recorded simultaneously. The angle of incidence of the light was kept at 55°, i.e., the magic angle to avoid orientation effects on the π^* state intensity,[17] except when performing angle-dependent studies.

Nanoindentation experiments were made using a Nano Indenter® II. The load-displacement data obtained were analyzed using the method of Oliver and Pharr.[18] Each sample was indented at nine different depths, at a constant rate of 10% of the maximum depth per second. Each unloading was terminated at 10% of the peak load to ensure that contact was maintained between specimen and indenter. Each indentation

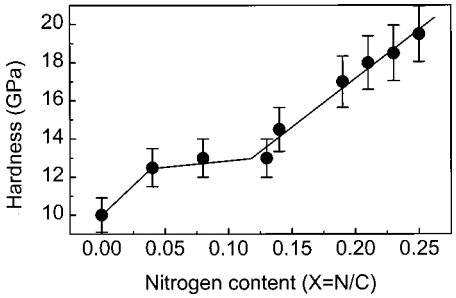

FIG. 1. Hardness of a set of carbon nitride films determined by nanoindentation measurements, as a function of the nitrogen content.

experiment was performed ten times, with a hardness dispersion below 8%. The hardness of a film was assigned to the value corresponding to a penetration depth ~10% of the film thickness.

Figure 1 displays the hardness of the different films as a function of the nitrogen content. The nitrogen fraction $X=[\mathrm{N}]/[\mathrm{C}]$ was directly computed from the intensity of the XANES spectra shown below, and is in agreement with the values derived from complementary photoemission and ion-scattering measurements. The hardness of the carbon nitride films with $X<0.13$ is independent of the nitrogen content, although is ~25% larger than for the plain carbon film. However, for $X>0.13$ the hardness increases linearly with the nitrogen content up to ~20 GPa for the composition range studied. This behavior suggests changes in the bonding structure of the films with the nitrogen content, that we have followed by x-ray-absorption spectroscopy.

Figure 2 displays the C(1s) and N(1s) XANES spectra from a set of carbon nitride films with different nitrogen contents. The spectra are shown normalized to the maximum height for comparison purposes. Regarding the C(1s) XANES spectra, the presence of C-N bonds of π character

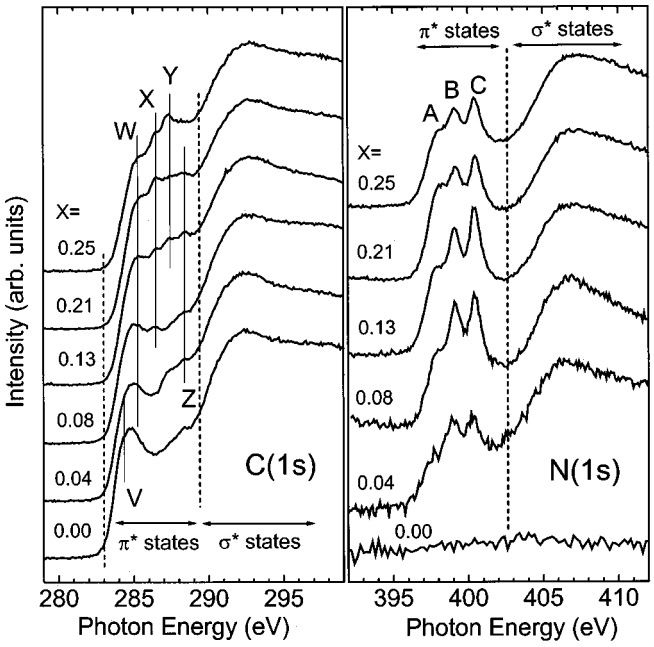

FIG. 2. C(1s) and N(1s) XANES spectra from a set of carbon nitride films with different nitrogen content $X=[\mathrm{N}]/[\mathrm{C}]$.

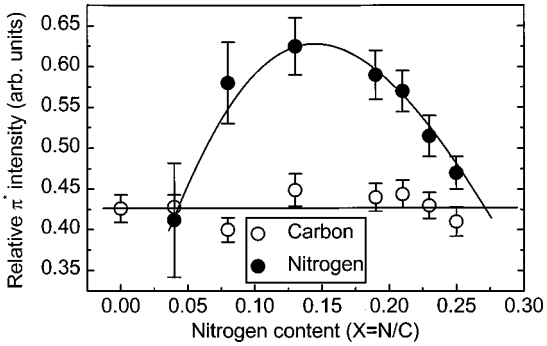

FIG. 3. Intensity of π^* states relative to the σ^* states in the XANES spectra from carbon and nitrogen atoms.

is revealed by the shift of the absorption threshold to higher energies with increasing nitrogen content due to charge transfer to the more electronegative N atoms, and by the appearance of several peaks in the 285–290-eV region, labeled as $V-Z$ in Fig. 2. These peaks originate from the different bonding environments of the carbon atoms, though a definitive assignment is still lacking. Similar features, although with different relative intensities, have been reported in previous studies.[13–16] Regarding the N(1s) XANES spectra, the presence of three well-resolved peaks, labeled as $A-C$, in the 396–402-eV range indicates π^* bonding in three different chemical environments. This three-peak structure has been observed by other groups[16,19] and seems typical of carbon nitride films with an [N]/[C] ratio below 0.4. For higher nitrogen content, the N(1s) XANES contains a single broad π^* peak[13,14] that can be understood from the merging of the three peaks observed here for low nitrogen concentrations.[15]

To study the electric charge contribution of carbon and nitrogen atoms to π bonding, we have computed the intensity of the whole π^* region relative to the σ^* intensity for each spectrum, and the values are displayed in Fig. 3. The limits of integration to compute the π^* intensity are not crucial, as long as one includes the whole π^* region. To compute the σ^* intensity it is enough not to overlap with the π^* states. Changing the limits of integration within these constraints always yields a similar result within a proportionality factor. To keep the scale factors as similar as possible for C and N, the same energy interval of integration is considered for both π^* and σ^* states.

For the C(1s) spectra, the proportion of π^* states was computed from the ratio of the area between 282 and 289 eV, representing π^* states, to the area between 292 and 299 eV, representing σ^* states. The relative C(1s) π^* intensity remains constant within 5% for the whole composition range and is the same as that for the evaporated carbon film represented in the bottom spectrum ($X=0$), which is composed of ~100% sp^2 carbon.[20] Therefore, formation of sp^3 sites does not take place and the hardness increase cannot be related to formation of sp^3 carbon cross-linking sites. For the N(1s) spectra, however, a variation of ~50% takes place as is displayed in Fig. 3. The N(1s) π^* intensity was computed from the ratio of the area between 396 and 402 eV, representing π^* states, to the area between 405 and 411 eV, representing σ^* states. The N(1s) π^* intensity increases with nitrogen content until reaching a maximum around $X=\frac{1}{6}$ and

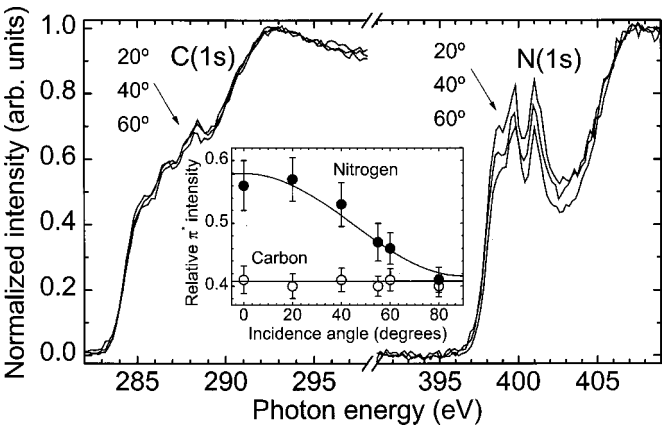

FIG. 4. XANES spectra for different angles of incidence of the light. Inset: dependence of the relative π^* intensity with the incidence angle.

decreases for larger nitrogen content.

Previous work simply relates the π^* intensity to the number of atoms with sp^2 hybridization. However, a change in the bonding angle would result also in a variation of the electric charge contributing to π bonding. The maximum charge density in π bonds will occur when the three σ bonds lie in a basal plane, and it will decrease when the σ bonds are not coplanar.[7] This is well known from model molecules like pyrrole, where the three coplanar sp^2 hybrid orbitals of nitrogen form three σ bonds and the remaining two p electrons in the lone orbital are delocalized with a partial flow of charge ($\sim 0.2e$) away from the nitrogen.[21] In this way, nitrogen participates in π bonding and exhibits π^* unoccupied states that can be observed by XANES spectroscopy.[22] When the ring is not planar, the lone pair is not accurately of π type and conjugation with the ring is inhibited.[23]

The observation of the increase of the N($1s$) π^* intensity with the nitrogen content for $X<\frac{1}{6}$ can be explained by a transition from nonplanar to planar nitrogen bonding geometry when the composition of one nitrogen atom per ring is approached. The subsequent decrease observed for $X>\frac{1}{6}$ can be explained by two different factors: (1) an increasing corrugation of the basal planes, and (2) cross-linking of curved basal planes through nonplanar nitrogen. The latter point has been previously proposed as a plausible explanation of the mechanical properties of graphitic carbon nitride films.[11] The present XANES results clearly indicate that only the nitrogen atoms can act as the linking sites of different basal planes in a cross-linking geometry.

Finally, we search for information on the orientation of the basal planes by angle-dependent XANES, since the intensity of π^* states follows a cosine-squared dependence with the angle between the light and the π bonds.[17] This can be used to detect the texture of graphitic films, even when long-range order is lacking.[24] The measurements were performed on the sample with the largest nitrogen content, $X=0.25$, and the results are shown in Fig. 4. The spectra are normalized to the maximum intensity and were measured with different angles of incidence of the synchrotron light. The inset displays the dependence of the relative π^* intensity with the incidence-angle curve fitted to a $\cos^2\theta$ law. The N($1s$) signal shows an anisotropy of ~ 0.2, which is absent in the C($1s$) signal. The anisotropy of the N($1s$) π^* signal

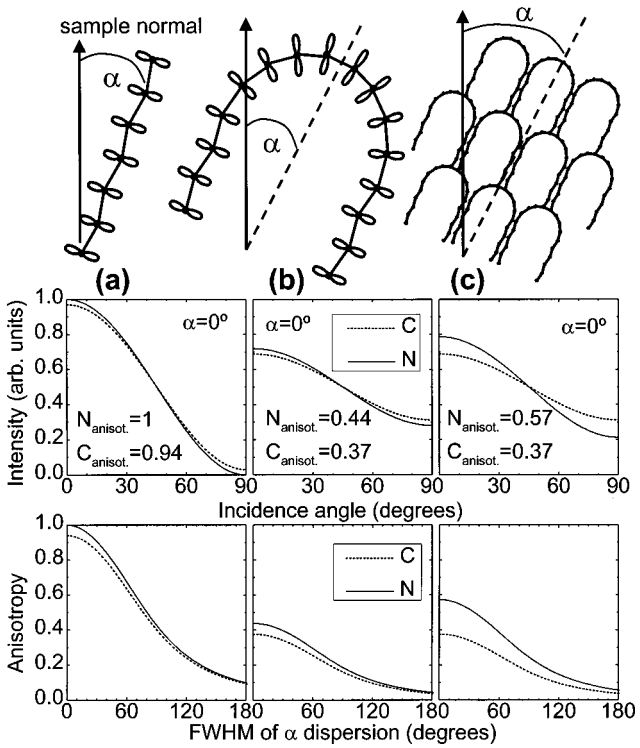

FIG. 5. Geometrical models representing side views of the basal planes, and the calculated anisotropy of the XANES signal at the C and N edges for each model. The central panels represent a perfect orientation of the model structures and the bottom panels correspond to a Gaussian distribution of the misorientation angle α.

corresponds to a preferential orientation of the nitrogen p orbitals parallel to the surface, i.e., basal planes perpendicular to the surface, as has been observed in other ion beam grown films.[24]

The distinct angular behavior of the C and N signal cannot be explained for flat basal planes. To verify if corrugation, folding, and cross-linking of basal planes can account for the observed behavior, we perform an analysis of the π^*-state anisotropy for simple geometries. The models are displayed in the top panel of Fig. 5 as side views of the basal planes, forming a misorientation angle α with the sample normal. The nitrogen atoms are represented with black dots and a figure-eight shape sketching the orientation of their p orbitals. The segments represent a section of carbon flat basal planes. The bending angle at a nitrogen atom will depend on the nitrogen hybridization, ranging from 0° for pure sp^2 to 19.5° for pure sp^3. For simplicity we consider in Fig. 5 an intermediate 10° angle, without losing generality.

The central panels of Fig. 5 represent the predicted angular dependence of the π^* intensity at the C and N edges for each model, assuming a perfect orientation with $\alpha=0°$. The displayed values of the anisotropy correspond to the maximum intensity change. The bottom panels of Fig. 5 represent the dependence of the C and N π^* anisotropy with the disorder of the structure. This is modeled with a Gaussian distribution of α angles centered in $\alpha=0$, with a certain full width at half maximum (FWHM).

Model (a) represents a corrugated plane, accounting for a 6% larger anisotropy of the nitrogen signal compared to the

carbon signal. Model (b) considers a curved plane, that yields a ~17% larger anisotropy of the N signal compared to the C signal. Model (c) considers a periodic structure of curved basal planes, linked through nitrogen atoms that do not contribute to π bonding. In this case the N anisotropy is ~45% larger than for C. However, for perfectly oriented structures the carbon anisotropy remains large. Assuming a certain disorder of the structure, as shown in the bottom panels of Fig. 5, the signal anisotropy is reduced. In this way, the C anisotropy can get too small to be detected, while the N anisotropy is still appreciable. This situation is found in model (c) for a FWHM of $\alpha \sim 100°$.

In summary, our experimental results indicate the distinct behavior of p electrons from carbon and nitrogen atoms regarding the formation of π bonds in graphitic carbon nitride with $[N]/[C] < 0.3$. The density of the π^* states from carbon atoms remains constant over the whole composition range and corresponds to ~100% sp^2 hybridized carbon. Therefore, any model of basal planes cross-linking through sp^3-hybridized carbon atoms is ruled out. The density of π^* states from nitrogen atoms is maximum for $[N]/[C] \sim 1/6$, and decreases for higher nitrogen content. The decrease is related to the curvature of basal planes and cross-linking through nonplanar nitrogen atoms, in agreement with the angular dependence of the XANES signal. Cross-linking explains the hardness increase with the nitrogen content. The distinct behavior of π^* states from C and N should be directly comparable with the electronic structure predicted by theoretical models of graphitic carbon nitride.

This work has been partially financed by the Spanish CICYT under projects MAT99-0830 and by the BRITE-EURAM contract BRPR-CT97-0487. We are indebted to P. Parent and C. Laffon for their help with the XANES measurements. The synchrotron work was financed by the TMR program of the European Union. Grants from the CAM and FPI-MEC programs of Spain are appreciated.

[1] A. Y. Liu and M. L. Cohen, Science **245**, 841 (1989).
[2] C. Ronning, H. Feldermann, R. Merk, H. Hofsäss, P. Reinke, and J. U. Thiele, Phys. Rev. B **58**, 2207 (1998).
[3] M. Côté, J. C. Grossman, M. L. Cohen, and S. G. Louie, Phys. Rev. B **58**, 664 (1998); G. Jungnickel, P. K. Sitch, Th. Fraumheim, B. R. Eggen, M. I. Heggie, C. D. Latham, and C. S. G. Cousins, *ibid.* **57**, R661 (1998); J. E. Lowther, *ibid.* **59**, 11 683 (1999).
[4] F. Weich, J. Widany, and Th. Frauenheim, Phys. Rev. Lett. **78**, 3326 (1997).
[5] J. E. Lowther, Phys. Rev. B **57**, 5724 (1998).
[6] S. Souto, M. Pickholz, M. C. dos Santos, and F. Alvarez, Phys. Rev. B **57**, 2536 (1998).
[7] M. C. dos Santos and F. Alvarez, Phys. Rev. B **58**, 13 918 (1998).
[8] H. Sjöström, S. Stafström, M. Boman, and J. E. Sundgren, Phys. Rev. Lett. **75**, 1336 (1995).
[9] I. Alexandrou, H. J. Scheibe, C. J. Kiely, A. J. Papworth, G. A. J. Amaratuga, and B. Schultrich, Phys. Rev. B **60**, 10 903 (1999).
[10] N. Hellgren, M. P. Johansson, E. Broitman, L. Hultman, and J. E. Sundgren, Phys. Rev. B **59**, 5162 (1999).
[11] B. C. Holloway, O. Kraft, D. K. Shuh, M. A. Kelly, W. D. Nix, P. Pianetta, and S. Hagström, Appl. Phys. Lett. **74**, 3290 (1999).
[12] D. Marton, K. J. Boyd, A. H. Al-Bayati, S. S. Todorov, and J. W. Rabalais, Phys. Rev. Lett. **73**, 118 (1994).
[13] B. C. Holloway, D. K. Shuh, M. A. Kelly, W. Tong, J. A. Carlisle, I. Jimenez, D. G. J. Sutherland, L. J. Terminello, P. Pianetta, and S. Hagström, Thin Solid Films **290/291**, 94 (1996).
[14] S. Lopez, H. M. Dunlop, M. Benmalek, G. Tourillon, M. S. Wong, and W. D. Sproul, Surf. Interface Anal. **25**, 827 (1997).
[15] I. Jiménez, W. M. Tong, D. K. Shuh, B. C. Holloway, M. A. Kelly, P. Pianetta, L. J. Terminello, and F. J. Himpsel, Appl. Phys. Lett. **74**, 2620 (1999).
[16] J. M. Ripalda, E. Román, N. Díaz, L. Galán, I. Montero, and G. Gomelli, Phys. Rev. B **60**, R3705 (1999).
[17] J. Stöhr, *NEXAFS Spectroscopy* (Springer, Berlin, 1992).
[18] W. C. Oliver and G. M. Pharr, J. Mater. Res. **7**, 1564 (1992).
[19] C. Quirós, L. Soriano, G. G. Fuentes, E. Elizalde, P. R. Bressler, and J. M. Sanz, BESSY Jahresbericht 1998 (unpublished), p. 381; M. Lübbe, S. Park, P. R. Bressler, W. Braun, and D. R. T. Zahn, BESSY Jahresberich 1998 (unpublished), p. 378.
[20] J. Robertson, Adv. Phys. **35**, 317 (1986).
[21] R. L. Miller, P. G. Lykos, and H. N. Schmeising, J. Am. Chem. Soc. **84**, 4623 (1962).
[22] Q. Zhu, S. L. Money, A. E. Russell, and K. M. Thomas, Langmuir **13**, 2149 (1997).
[23] Roy McWeeny, *Coulson's Valence* (Oxford University Press, Oxford, 1979).
[24] I. Jiménez, M. M. García, J. M. Albella, and L. J. Terminello, Appl. Phys. Lett. **73**, 2911 (1998); I. Jiménez, A. F. Jankowski, L. J. Terminello, D. G. J. Sutherland, J. A. Carlisle, G. L. Doll, W. M. Tong, D. K. Shuh, and F. J. Himpsel, Phys. Rev. B **55**, 12 025 (1997).